Journal of Hazardous Materials 161 (2009) 677–685

Contents lists available at ScienceDirect

Journal of Hazardous Materials

journal homepage: www.elsevier.com/locate/jhazmat

Removal of lead ions by acid activated and manganese oxide-coated bentonite

E. Eren [a,*], B. Afsin [b], Y. Onal [c]

[a] Ahi Evran University, Faculty of Arts and Science, Department of Chemistry, 40100 Kırsehir, Turkey
[b] Ondokuz Mayis University, Faculty of Arts and Science, Department of Chemistry, 55139 Kurupelit/Samsun, Turkey
[c] Inonu University, Faculty of Engineering, Department of Chemical Engineering, 44280 Malatya, Turkey

ARTICLE INFO

Article history:
Received 19 November 2007
Received in revised form 3 April 2008
Accepted 3 April 2008
Available online 11 April 2008

Keywords:
Bentonite
Adsorption
Thermodynamic
Manganese oxide
Lead

ABSTRACT

This paper presents the adsorption of Pb(II) from aqua solutions onto Unye (Turkey) bentonite in raw (RB), acid activated (AAB) and manganese oxide-coated (MCB) forms. Adsorption of Pb(II) by RB, AAB and MCB sample was investigated as a function of the initial Pb(II) concentration, solution pH, ionic strength, temperature and inorganic ligand (Cl^-). Changes in the surfaces and structure were characterized by means of XRD, IR and potentiometric titration. The Langmuir monolayer adsorption capacities of RB, AAB and MCB in 0.1 M KNO_3 solution were estimated as 16.70, 8.92 and 58.88 mg/g, respectively. The spontaneity of the adsorption process is established by decrease in ΔG which varied from −21.60 to −28.60 kJ/mol (RB), −22.63 to −29.98 kJ/mol (AAB) and −19.57 to −26.22 (MCB) in temperature range 303–338 K.

1. Introduction

Heavy-metal pollution occurs in many industrial wastewater such as those produced by metal plating facilities, mining operations, battery manufacturing process, the production of paints and pigments, and the glass production industry. Lead can enter the human body through inhalation, skin contact or with diet, and can produce adverse effects on virtually every system in the body. Low levels of Pb(II) have been identified with anemia while high levels cause severe dysfunction of the kidneys, liver, the central and peripheral nervous system, the reproductive system, and high blood pressure. The most severe neurological effect of lead in adults is lead encephalopathy, which is a general term to describe various diseases that affect brain function. The lower IQ values and other neuropsychological deficits among the children exposed to higher lead levels have been well documented [1]. Therefore, the heavy-metal levels in wastewater, drinking water, and water used for agriculture should be reduced to the maximum permissible concentration. Several methods have been applied over the years for the elimination of these metal ions present in industrial wastewaters and soils. Conventional technologies for the removal of heavy metal such as chemical precipitation, electrolysis, ion exchange and reverse osmosis are often neither effective nor economical. Among the physico-chemical treatment process adsorption is highly effective, cheap and easy to adapt [2]. Adsorption has been proven to be a successful method for removal of heavy metals from wastewater. Activated carbon is highly effective in adsorbing heavy metals from wastewater but high cost limits its use. Due to the high abundance and their low cost, clay minerals are a strong candidate as an adsorbent for removal of heavy metal from wastewater.

Bentonite is a natural clay mineral that is found in many places of the world. Any clay of volcanic origin that contains montmorillonite is referred to as bentonite. It belongs to the 2:1 clay family, the basic structural unit of which is composed of two tetrahedrally coordinated sheets of silicon ions surrounding a sandwiched octahedrally coordinated sheet of aluminum ions. The isomorphous substitution of Al^{3+} for Si^{4+} in the tetrahedral layer and Mg^{2+} or Fe^{3+} for Al^{3+} in the octahedral layer results in a net negative surface charge on the clay [3]. Compared with other clay types, it has excellent adsorption properties and possesses adsorption sites available within its interlayer space as well as on the outer surface and edges [4]. Adsorption of metal ions onto montmorillonite appears to involve two distinct mechanisms: (i) an ion exchange reaction at permanent-charge sites, and (ii) formation of complexes with the surface hydroxyl groups [5].

A composite adsorbent, manganese oxide-coated bentonite (MCB), was proposed and studied in this research. The reason for choosing manganese oxides is that relative to Fe or Al oxides, manganese oxides have a higher affinity for many heavy metals [6]. Bentonite, which has a high surface area, should provide an efficient surface for the manganese oxide. At the same time, the manganese oxides can improve the heavy-metal adsorption

* Corresponding author. Tel.: +90 386 211 45 00; fax: +90 386 211 45 25.
E-mail address: erdalern@omu.edu.tr (E. Eren).

0304-3894/$ – see front matter © 2008 Elsevier B.V. All rights reserved.
doi:10.1016/j.jhazmat.2008.04.020

Nomenclature

RB	raw bentonite
AAB	acid activated bentonite
MCB	manganese oxide-coated bentonite
m	mass of adsorbent (g/l)
q_e	amount of adsorbate removed from aqueous solution at equilibrium (mg/g)
C_e	equilibrium concentration of the adsorbate in the solution (mg/l)
q_m	mass of adsorbed solute completely required to saturate a unit mass of adsorbent (mg/g)
K_L	constant that represents the energy or net enthalpy of adsorption (l/mg)
K_F	Freundlich constant indicative of the adsorption capacity of the adsorbent (mg/g)
n	experimental constant indicative of the adsorption intensity of the adsorbent.
IS	ionic strength

capacity of bentonite. The objective of this study is to investigate comparative adsorption characteristics for removal of Pb(II) from aqueous solution by the use of raw bentonite (RB), acid activated bentonite (AAB) and manganese oxide-coated bentonite. The influence of pH, ionic strength, ligand (Cl^-) and temperature on the adsorption of Pb(II) by the RB, AAB and MCB samples was investigated to better understand the Pb(II) adsorption process.

2. Experimental

2.1. Reagents

All reagents used were of analytical purity. Synthetic solutions were prepared from concentrated stock solutions (Merck). A stock solution of Pb(II) was prepared by dissolving required amount of $Pb(NO_3)_2$ (Merck) in double distilled water. Reagent grade H_2SO_4 (Merck) was used for acid activation. HNO_3 and NaOH were obtained from Merck and used for pH value adjustment. Other agents used, such as NaCl, $NaNO_3$, Na_2SO_4, Na_3PO_4, $MnCl_2$ were all of analytical grade and all solutions were prepared with double distilled water.

RB had a mineral composition of 76% montmorillonite, 8% quartz, 12% dolomite and 4% other minerals. Whiteness was found to be 85%. RB was composed of 62.70% SiO_2, 20.10% Al_2O_3, 2.16% Fe_2O_3, 2.29%CaO, 3.64% MgO, 0.27%, Na_2O, 2.53% K_2O, 0.21% TiO_2, P_2O_5% 0.02. The ignition loss of the RB at 1273 K was also found to be 6.1%. The cation exchange capacity (CEC), determined with triethanolamine-buffered $BaCl_2$ solution (c = 0.1 M) followed by a reexchange with aqueous $MgCl_2$ solution (c = 0.1 M), is of 0.65 mmol/g [7], and the major exchangeable cations are: Ca (57.1%), Mg (28.8%), Na (10.5%) and K (3.8%).

2.2. Preparation and characterization of RB, AAB and MCB

2.2.1. Preparation of RB

The RB sample (from Unye, Turkey) was ground and washed in deionized water several times at a 1:10 bentonite/water ratio. The mixture was stirred for 3 h and then kept standing overnight, followed by separation, washing and drying at 60 °C.

2.2.2. Preparation of AAB

20 g RB was mixed with 25 ml of 2.0 M H_2SO_4 solution at 90 °C, and stirred 3 h. Afterward, the sample solution was first cooled to room temperature, then filtered off using centrifugal separator and washed sequentially with deionized water 3 times to remove the ions and other residues. The resulting products were finally dried at 105 °C for 24 h, and stored in the desiccator.

2.2.3. Preparation of MCB

Manganese chloride and sodium hydroxide were mainly used in the modification of RB to enhance the adsorption capacity of RB. 20 g of RB were immersed in sufficient 2.0 M sodium hydroxide and temperature of the reaction mixture was maintained at 90 °C for 4 h. The base activated RB was dispersed into 150 ml of 0.1 M $MnCl_2$ aqueous solution. 300 ml of 0.1 M NaOH aqueous solution was added slowly with a drop rate 1 ml/h. The titration was carried out under nitrogen flow throughout the procedure to minimize unexpected reactions, e.g. formation of carbonate salts. The obtained powder was rinsed with 0.01 M HCl aqueous solution to remove the excess $Mn(OH)_2$ precipitated on the outer surface of the clay and further washed with deionized water. The oxidation was performed in aqueous suspension system at room temperature. The $Mn(OH)_2$ intercalated compound prepared as above was dispersed in 50 ml of 1.5 M H_2O_2 basic solution and vigorously stirred. The color of the sample immediately turned from original light color to dark brown, indicating the oxidation of the hydroxide into oxide phase. For equilibrium, the suspension was further stirred for 24 h. The powder sample was washed with deionized water and dried at 60 °C [8].

The mineralogical compositions of the RB and MCB samples were determined from the X-ray diffraction (XRD) patterns of the products taken on a Rigaku 2000 automated diffractometer using Ni filtered Cu Kα radiation. XRD analysis of the bentonite was performed using the three-principal lines [9]. IR spectra of the bentonite samples were recorded in the region 4000–400 cm^{-1} on a Mattson-1000 FTIR spectrometer at 4 cm^{-1} resolution. Surface areas were measured by nitrogen adsorption at 77 K using Quantachromosorb. Moisture and gases on the solid surface or penetrated in the open pores were removed by heating at 120 °C for 24 h prior to the surface area measurements. The values determined for the RB, AAB and MCB were 36, 110 and 64 m^2/g, respectively.

2.3. Adsorption dependence on Pb(II) concentration

The adsorption of Pb(II) by bentonite samples was performed by a batch equilibrium technique at room temperature. Briefly, 0.050 g of bentonite sample and 20 ml of $Pb(NO_3)_2$ solution were added in 50 ml polypropylene centrifuge tubes. Ionic strength controlled at 0.1 M KNO_3 and the pH of the system was maintained at 6.0. The initial Pb(II) concentrations varied from 0.01 to 1.0 mM. A 24-h contacting period was found to be sufficient to achieve equilibrium. The samples were allowed to equilibrate for 24 h, centrifuged at 4500 × g for 20 min and then filtered. The adsorbed amounts of metals were calculated by the difference between the initial and final concentrations remaining in the equilibrium filtrate after adsorption. All the measurements were made in duplicate. For each sample, an experiment without adsorbent was performed to test possible adsorption and/or precipitation of metals onto the container walls. Preliminary experiments showed that metal losses due to the adsorption onto the container walls and to the filter paper were negligible. The adsorption isotherm experiments were repeated in triplicate and the average values were reported. Adsorbed Pb(II) was calculated from the difference between the Pb(II) initially added to the system and that remaining in the solution after equilibration by a Unicam 929 model flame atomic absorption spectrophotometer, Pb(II): lamp current 10 mA, wavelength 217.1 nm, slit width 0.5 nm, optimum working range 2–10.0 μg/ml; flame type air/acetylene, fuel flow rate 1.2 l/s. The dilutions induced by the pH

controls were considered while computing the amount of Pb(II) adsorbed.

2.4. Effect of ionic strength, pH, inorganic ligand and temperature

Adsorption experiments were carried out in polyethylene test tubes at 23 ± 2 °C by using the batch technique. The reaction mixture consisted of a total 50 ml containing 2g/l adsorbent and the desired concentration of Pb(II) ions. A solution of 1.0 mM Pb(II) was prepared from $Pb(NO_3)_2$ by dissolving in deionized water. The stock was diluted to prepare a working solution of 0.5 mM Pb(II). The background electrolyte solutions were 0.01, 0.05, and 0.1 M KNO_3. Solution pH was adjusted with 0.1 M HNO_3 or 0.1 M NaOH, such that the equilibrium solutions had pH values ranging from 3.0 to 6.5. Preliminary kinetic studies indicated that Pb(II) adsorption was characterized by a rapid initial adsorption (within 1 h) followed by a much slower, continuous uptake. A 24-h contacting period was found to be sufficient to achieve equilibrium. The separation of the liquid from the solid phase was achieved by centrifugation at 4500 rpm for 20 min. Pb(II) adsorption in the presence of Cl^- was performed by equilibrating 0.05 g of bentonite sample in 20 ml of 0.25 M KNO_3 background electrolyte, 10 ml of Pb(II) working solution, and 20 ml of a NaCl working solution (achieving 0.01 M Cl^-) in 50-ml polyethylene test tubes. These experiments were performed in duplicate. The temperature was varied from 303 to 338 K at a constant pH of 6.0. For these experiments, 2 g/l of bentonite samples with 20.7 mg/l Pb (II) solutions was employed.

3. Results and discussion

3.1. Data processing

The adsorption capacity of Pb(II) ions adsorbed per gram adsorbent (mg/g) was calculated using the equation

$$q_e = (C_0 - C_e)\frac{V}{m} \quad (1)$$

The adsorption percentage of Pb(II) ions was calculated by the difference of initial and final concentration using the equation expressed as follows:

$$R = \frac{C_0 - C_e}{C_0} \times 100 \quad (2)$$

where q_e is the equilibrium concentration of Pb(II) on the adsorbent (mg/g), C_0 the initial concentration of the Pb(II) solution (mg/l), C_e the equilibrium concentration of the Pb(II) solution (mg/l), m the mass of adsorbent (g), V the volume of Pb(II) solution (l), R the retention of Pb(II) in % of the added amount.

The adsorption isotherm indicates how the adsorption molecules distribute between the liquid phase and the solid phase when the adsorption process reaches an equilibrium state. The analysis of the isotherm data by fitting them to different isotherm models is an important step to find the suitable model that can be used for design purpose. There are several isotherm equations available for analyzing experimental adsorption equilibrium data. In this study, the equilibrium experimental data for adsorbed Pb(II) on bentonite sample were analyzed using the Langmuir, Freundlich and Dubinin–Radushkevich (D–R) isotherm models. These isotherms are as follows:

(a) Langmuir isotherm model [10]:

$$\frac{C_e}{q_e} = \frac{C_e}{q_m} + \frac{1}{K_L q_m} \quad (3)$$

where C_e is equilibrium concentration of Pb(II) (mg/l) and q_e is the amount of the Pb(II) adsorbed (mg) by per unit of bentonite (g). q_m and K_L are the Langmuir constants related to the adsorption capacity (mg/g) and the equilibrium constant (l/mg), respectively.

(b) Freundlich isotherm model [11]:

$$\log q_e = \log K_F + \left(\frac{1}{n}\right)\log C_e \quad (4)$$

where K_F and n are Freundlich constants related to adsorption capacity and adsorption intensity, respectively.

(c) D–R isotherm model [12–16]:

$$\ln q_e = \ln q_m - \beta\varepsilon^2 \quad (5)$$

where β is the activity coefficient related to mean adsorption energy (mol^2/J^2) and ε is the Polanyi potential ($\varepsilon = RT\ln(1 + (1/C_e))$). The D–R isotherm is applied to the data obtained from the empirical studies. The mean adsorption energy, E (kJ/mol) is as follows:

$$E = \frac{1}{\sqrt{-2\beta}} \quad (6)$$

This adsorption potential is independent of the temperature, but it varies depending on the nature of adsorbent and adsorbate.

Using the following equations, the thermodynamic parameters of the adsorption process can be determined from the experimental data:

$$\ln K_d = \frac{\Delta S}{R} - \frac{\Delta H}{RT} \quad (7)$$

$$\Delta G = \Delta H - T\Delta S \quad (8)$$

$$K_d = \frac{q_e}{C_e} \quad (9)$$

where K_d is the distribution coefficient for the adsorption, ΔS, ΔH and ΔG are the changes of entropy, enthalpy and the Gibbs energy, q_e is the equilibrium concentration of Pb(II) on the adsorbent (mg/kg), T (K) is the temperature, R (J mol^{-1} K^{-1}) is the gas constant, The values of ΔH and ΔS were determined from the slopes and intercepts of the plots of $\ln K_d$ vs. $1/T$.

3.2. Material characterization

The XRD patterns of RB and MCB samples were presented in Fig. 1. For the XRD pattern of RB, one reflection was observed in the region $2^\circ < 2\theta < 8^\circ$ (Fig. 1a). This corresponds to the 5.76 (2θ) value from which the interlamellar distance was found to be 15.33 Å. The position of d_{001} peak of AAB sample shifted from 15.33 to 16.98 Å (Fig. 1b) which was accompained by an intensity decrease from 100 to 47% (Table 1). The XRD results also show that acid activation has caused structural changes in the AAB. Activation has affected mainly the 001 reflection; the intensities of the 001, 003 and 060 reflections have been reduced, while the intensities of the 020 and 006 reflections have been increased significantly by the

Table 1
d-spacing and intensity values of reflections for bentonite samples

Reflection	RB		AAB		MCB	
	d (Å)	Intensity	*d* (Å)	Intensity	*d* (Å)	Intensity
d_{001}	15.33	100	16.98	47	12.40	100
d_{003}	5.05	8	5.05	11	–	–
d_{020}	4.42	34	4.48	70	4.47	95
d_{101}	–	–	3.96	38	–	–
d_{006}	2.55	21	2.57	33	2.55	45
d_{060}	1.49	13	1.50	23	1.49	34

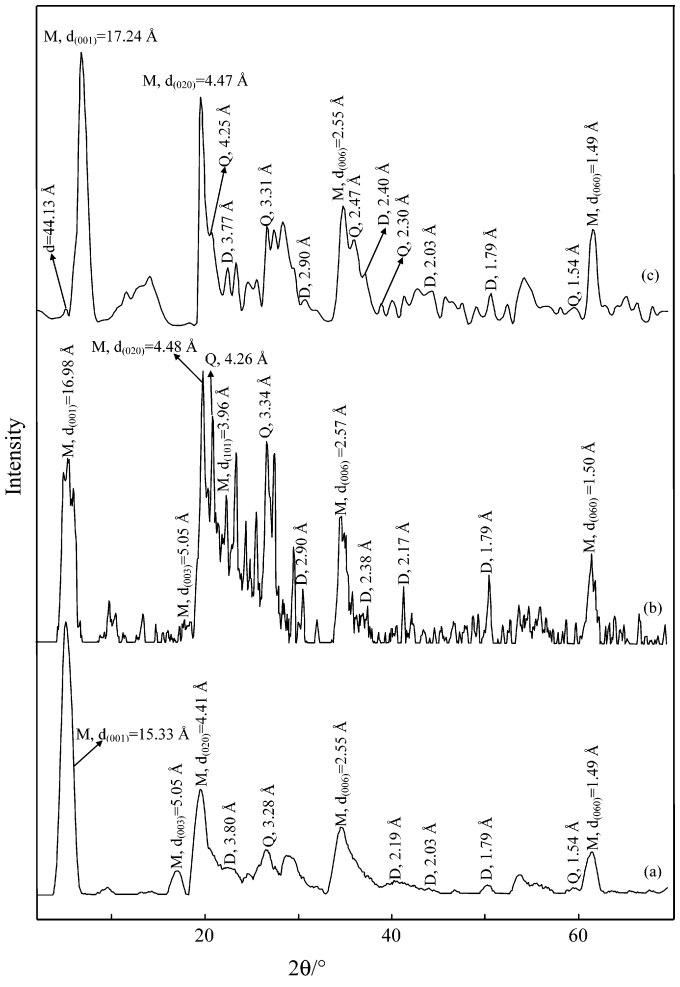

Fig. 1. The X-ray diffraction patterns of the RB (a), AAB (b) and MCB (c) samples (M: montmorillonite, Q: Quartz, D: Dolomite).

acid activation process (Table 1). Acid activated sample displays an increase of the background in the interval between 20° and 30° due to the deposition of amorphous silica caused after the attack on the octahedral layer and the exposure of the tetrahedral layer. Acid activation of the RB yielded d_{101} reflection at 3.96 Å ($2\theta = 22.40$), which is absent in the RB. Appearance of new reflection indicate the formation of expansible phases and interlamellar expansion [17].

The XRD results also show that manganese oxide modification has caused structural changes in the MCB. The position of d_{001} peak of MCB sample shifted from 15.33 to 12.41 Å (Fig. 1c). The formation of a new structure was illustrated by the peak appearing at 44.13 Å ($2\theta = 5.12$) in the XRD pattern of the MCB. This new peak situated at lower 2θ value was likely to appear because of agglomeration of the MCB sheets [18]. Modification has affected mainly the 001 reflection; the intensities of the 020, 006 and 060 reflections have been increased significantly by the manganese oxide modification process (Table 1). MCB sample displays an increase of the background in the interval between 20° and 30°. The d_{003} reflection of RB at 5.05 Å ($2\theta = 17.52$) disappeared after modification process.

To better understand surface properties, potentiometric titrations were conducted. Fig. 2 shows proton adsorption curves performed at 0.1 M NaCl supporting electrolyte concentration for the RB and MCB samples. As shown in Fig. 2, the point of zero charge (pH_{PZC}) of RB is approximately 6.8. The MCB sample behaved similarly to MnO_2 where pH_{PZC} of MCB (3.5) is close to that of MnO_2

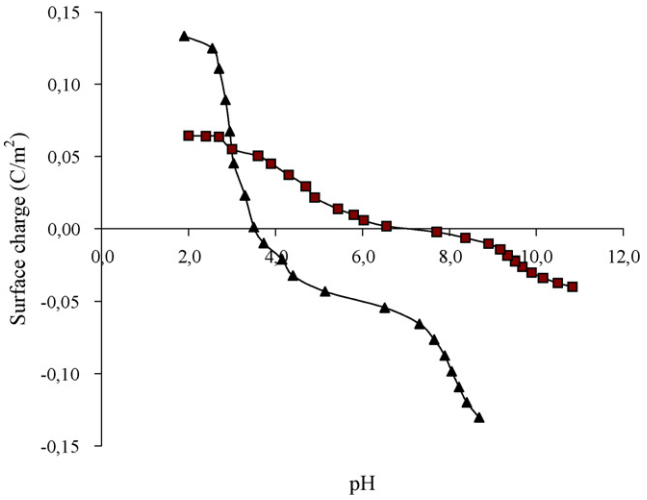

Fig. 2. Surface charge (C/m^2) vs. pH curves of bentonite samples in 0.1 M NaCl solution, squares, RB; triangles, MCB.

(2.4) [19]. The results suggest that the pH_{PZC} of MCB falls between the RB and MnO_2 and manganese oxide modification process play important role in surface charge behavior of the adsorbent.

Fig. 3a shows the infrared spectrum (IR) of the RB sample. The absorption band at 3635 cm^{-1} is due to stretching vibrations of structural OH groups of montmorillonite. The bands corresponding to AlAlOH, AlFeOH and AlMgOH bending vibrations were observed at 936, 885 and 845 cm^{-1}, respectively. A complex band at 1038 cm^{-1} is related to the stretching vibrations of Si–O groups, while the bands at 527 and 470 cm^{-1} are due to Al–O–Si and Si–O–Si bending vibrations, respectively. The band at 629 cm^{-1} was assigned to coupled Al–O and Si–O out-of-plane vibrations. The H_2O-stretching vibration was observed as a broad band at 3415 cm^{-1}. The shoulder near 3330 cm^{-1} is due to an overtone of the bending vibration of water observed at 1651 cm^{-1} [20,21]. The spectrum of AAB sample (Fig. 3b), has all absorption bands char-

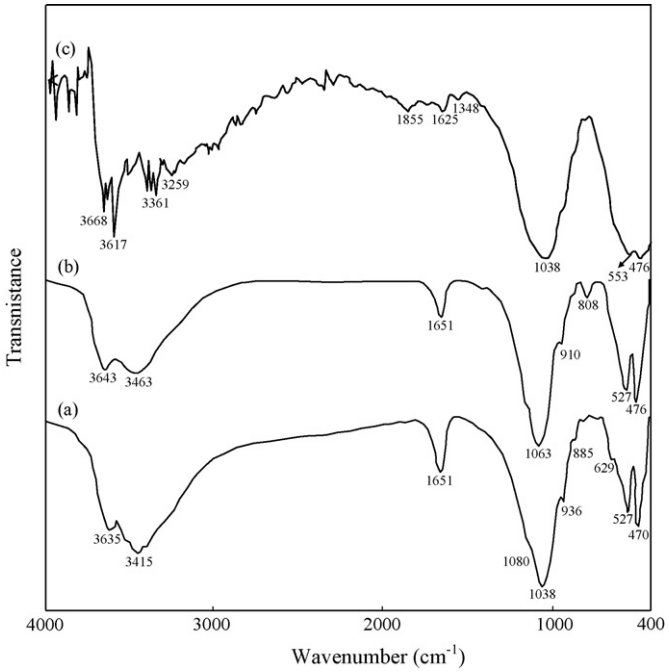

Fig. 3. IR spectra of the RB (a), AAB (b) and MCB (c).

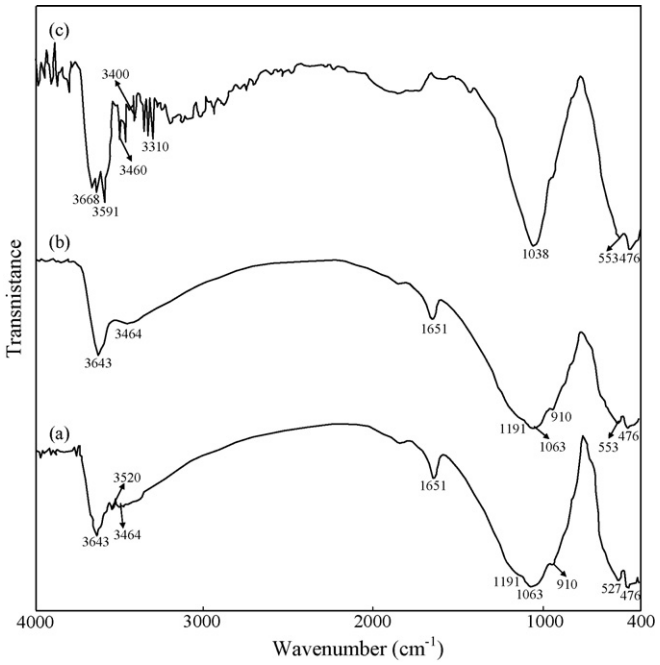

Fig. 4. IR spectra of the RB-Pb(II) (a), AAB-Pb(II) (b) and MCB-Pb(II) (c).

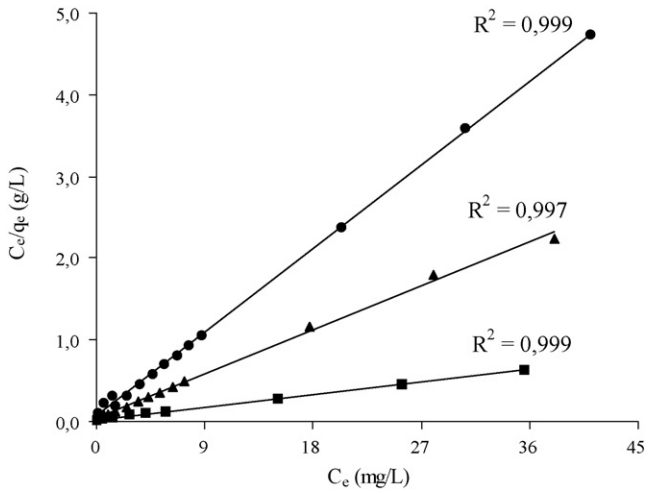

Fig. 5. Langmuir isotherm plots for the adsorption of Pb(II) onto the bentonite samples, RB; triangles, AAB; circles, MCB; squares. T = 303 K, initial pH 6.0, ionic strength (IS) is 0.1 (KNO_3).

acteristics of amorphous silica (1114, 808 and 476 cm^{-1}) confirms a high degree of structural decomposition [21]. Fig. 3c shows the IR spectrum of the MCB sample. Several absorption bands were observed at 3445, 1635, 1384, 1126, 577 and 535 cm^{-1}, respectively. The 3445 cm^{-1} band should be attributed to the O–H stretching vibration, and the 1625, 1348 bands are normally attributed to O–H bending vibrations combined with Mn atoms. The broad band at 553 should be ascribed to the Mn–O vibrations [22,23].

The IR spectra revealed the effect of Pb(II) on the lattice vibrational modes of montmorillonite (Fig. 4a–c). The IR spectra of Pb(II)-saturated bentonites have shown that Pb(II) ions locate into the clay lattice, and also affects Si–O vibrations in the 1200–950 cm^{-1} region [24–29]. Position of the Si–O bending vibration at 527 cm^{-1}, due to Si–O–Al remained basically unchanged for the Pb-RB, but some broadening and a decrease in intensity of the Si–O–Al band were observed (Fig. 4a). More distinct change of Si–O–Al band, moved to 553 cm^{-1}, broadened and decreased in intensity was found for the Pb-AAB (Fig. 4b). The position of the Mn–O bond vibration at 553 cm^{-1} remained basically unchanged for the MCB-Pb(II) sample, but some broadening and a decrease in intensity of this band was observed (Fig. 4c).

3.3. Adsorption isotherms and parameters

The equilibrium data for Pb(II) adsorption on bentonite samples were fitted to Langmuir equation (Eq. (3)): an equilibrium model able to identify the chemical mechanism involved. Linear plots of C_e/q_e vs. C_e (Fig. 5) were employed to determine the value of q_m (mg/g) and K_L (l/mg). The data obtained with the correlation coefficients (R^2) was listed in Table 2. The Langmuir monolayer adsorption capacity (q_m) gives the amount of the metal required to occupy all the available sites per unit mass of the sample. The Langmuir monolayer adsorption capacities of RB, AAB and MCB in 0.1 M KNO_3 solution were estimated as 16.70, 8.92 and 58.88 mg/g, respectively (Table 2). The Langmuir monolayer adsorption capacities of those in absence of KNO_3 solution were estimated as 64.29, 40.14 and 123.64 mg/g. As given in Section 2.2, the BET surface areas of RB and MCB are markedly lower than that of AAB, calculated q_m values indicate that surface area is not a crucial factor for the adsorption capacity of bentonites. As given in Table 2, the equilibrium constant values for RB, AAB and MCB were found to be 1.30, 1.58 and 0.59, respectively. The equilibrium constant values (K_L) suggest that the high-energy sites with high equilibrium constant had a significantly lower affinity than that for low-energy sites with low equilibrium constant. The high-energy sites on which Pb(II) was tightly held had a low adsorption maximum (q_m = 8.92 mg/g for ionic strength (IS) = 0.1 M KNO_3). The low-energy sites on which Pb(II) were loosely held had a high adsorption maximum (q_m = 58.88 mg/g for IS = 0.1 M KNO_3).

The adsorption capacities of the adsorbents for the removal of Pb(II) have been compared with those of other adsorbents reported in literature and the values of adsorption capacities have been presented in Table 3. The values are reported in the form of monolayer adsorption capacity. The experimental data of the present investigation are comparable with the reported values [29–33]. Comparison of maximum experimental adsorption capacities of Pb(II) for manganese oxide modified adsorbents were also given in Table 3 [31–33]. Maximum adsorption capacity of Pb(II) for the manganese oxide modified samples was approximately 2–4 times higher than that of the raw material. The Pb(II) adsorption capacities of diatomite and Mn-diatomite were determined as 24 and 99 mg/g, respectively [32]. In another study, Wang et al. [33] studied Mn oxide-coated carbon nanotube, for Pb(II) removal from aque-

Table 2
Langmuir and Freundlich isotherm parameters for the adsorption of Pb(II) onto bentonite samples in 0.1 M KNO_3 solution

Sample	Langmuir isotherm constants			Freundlich isotherm constants			D–R isotherm constants		
	q_m (mg/g)	K_L (l/mg)	R^2	n	K_f ((mg/g)(l/mg)$^{1/n}$)	R^2	q_m (mg/g)	E (kJ/mol)	R^2
RB	16.70	1.30	0.997	14.30	12.86	0.861	9.24	0.72	0.993
AAB	8.92	1.58	0.999	7.67	6.36	0.979	5.48	0.55	0.987
MCB	58.88	0.59	0.999	2.76	19.75	0.933	19.07	3.42	0.907

Table 3
Adsorption results of Pb(II) ions from the literature by various adsorbents

Adsorbent	Adsorption capacity (mg/g)	Ref. No
Natural bentonite	78.82	[29]
MX-80 bentonite	68.58	[14]
Montmorillonite	31.1	[30]
Manganese oxide-coated sand (303 K)	1.34	[31]
Diatomite (pH 5, 24 h)	24.0	[32]
Mn-diatomite (pH 5, 24 h)	99.0	[32]
Mn oxide-coated carbon nanotube (pH 5)	78.74	[33]
Carbon nanotube (pH 5)	≈26.24	[33]
RB (IS = 0)	64.29	In this study
RB (IS = 0.1 M KNO_3)	16.70	In this study
AAB (IS = 0)	40.14	In this study
AAB (IS = 0.1 M KNO_3)	8.92	In this study
MCB (IS = 0)	123.64	In this study
MCB (IS = 0.1 M KNO_3)	58.88	In this study

IS: Ionic strength (controlled by KNO_3).

ous solution. They reported that the carbon nanotube adsorbed Pb(II) with the adsorption capability of ≈26.24 mg/g. The capacity of the Mn oxide-coated carbon nanotube increased to 78.74 mg/g. The comparison of q_m value of MCB used in the present study with those obtained in the literature shows that MCB is more effective for this purpose (123.64 mg/g for IS = 0 and 58.88 mg/g for IS = 0.1). From these observations, it appears that the surface properties of raw bentonite could be improved upon modification of manganese oxide as previously reported by other researchers [31–33].

The equilibrium data also fitted to Freundlich equation (Eq. (4)), a fairly satisfactory empirical isotherm can be used for non-ideal adsorption. The Freundlich isotherm constants K_F and n are constants incorporating all factors affecting the adsorption process such as of adsorption capacity and intensity of adsorption. The constants K_F and n were calculated from Eq. (4) and Freundlich plots (Fig. 6). The values for Freundlich constants and correlation coefficients (R^2) for the different adsorbents used during the study are also presented in Table 2. Freundlich parameters (K_F and n) indicate whether the nature of adsorption is either favorable or unfavorable. The intercept is an indicator of adsorption capacity and the slope is an indicator of adsorption intensity. A relatively slight slope $n \ll 1$ indicates that adsorption intensity is favorable over the entire range of concentrations studied, while a steep slope ($n > 1$) means that adsorption intensity is favorable at high concentrations but much less at lower concentrations. In the adsorption systems, n

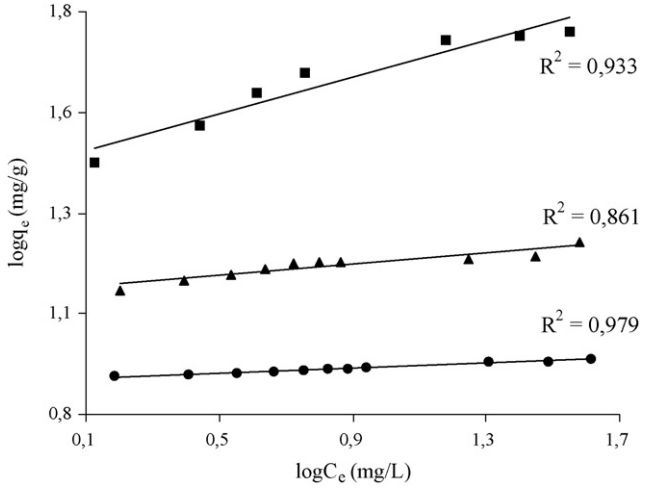

Fig. 6. Freundlich isotherm plots for adsorption of Pb(II) on the bentonite samples, RB; triangles, AAB; circles, MCB; squares. T = 303 K, initial pH 6.0, IS is 0.1 (KNO_3).

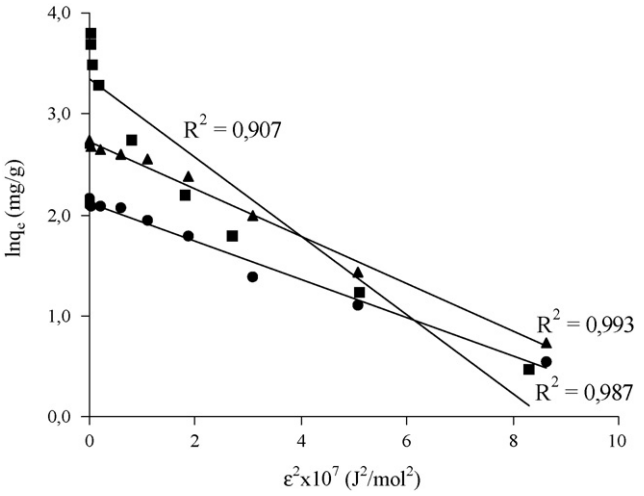

Fig. 7. D–R isotherm plot for adsorption of Pb(II) on the bentonite samples, RB; triangles, AAB; circles, MCB; squares. T = 303 K, initial pH 6.0, IS is 0.1 (KNO_3).

value is $n > 1$ which indicates that adsorption intensity is favorable over the entire range of concentrations studied. The K_F value of the Freundlich equation (Table 2) also indicates that MCB has a very high adsorption capacity for lead ions in aqueous solutions.

A plot of ln q_e against ε^2 is given in Fig. 7. D–R isotherm constants, q_m, for RB, AAB and MCB in 0.1 M KNO_3 solution were found to be 9.24, 5.48 and 19.07 mg/g, respectively (Table 2). The difference of q_m derived from the Langmuir and D–R models is large. The difference may be attributed to the different definition of q_m in the two models. In Langmuir model, q_m represents the maximum adsorption of metal ions at monolayer coverage, whereas it represents the maximum adsorption of metal ions at the total specific micropore volume of the adsorbent in D–R model. Thereby, the value of q_m derived from Langmuir model is higher than that derived from D–R model. The differences are also reported in previous studies [12,14]. The magnitude of E is used for estimating the type of adsorption mechanism. If the E value is between 8 and 16 kJ/mol, the adsorption process follows by chemical adsorption and if $E < 8$ kJ/mol, the adsorption process is of a physical nature [12–16]. The calculated values of E are 0.72, 0.55 and 3.42 kJ/mol for RB, AAB and MCB, respectively, and they are in the range of values for physical adsorption reactions. The similar results for the adsorption of Cr(III), Pb(II) and Zn(II) were reported by earlier workers [12,16].

3.4. Effect of ionic strength, pH and inorganic ligand

The adsorption of Pb(II) onto the bentonite samples as a function of ionic strength and pH was shown in Fig. 8a–c. The three bentonite samples showed an identical behavior of increased uptake of Pb(II) per unit mass with gradually increasing pH, and the shape of curves dependent on the bentonite surfaces. As shown in Fig. 8a, Pb(II) adsorption by the RB sample decreased when pH decreased. This result suggests that the adsorptive decrease was caused by the competition for exchange sites between H^+ and Pb(II) cations. At low pH there is also a decrease in Pb(II) adsorption with increasing ionic strength. The adsorption curve of AAB has a similar shape as that of RB sample (Fig. 8b). The adsorption curve for this sample is characterized by two distinct adsorption edges. For example, the first stage of adsorption edge commenced about 30% Pb(II) adsorption at pH ~3.0 and ended at pH ~4.0, at which about 38% of the total Pb(II) had been adsorbed in the presence of 0.1 M KNO_3. The second stage started at pH 4.0 and continued up to pH 5.5 where about 50% of the total Pb(II) was adsorbed. The adsorption of Pb(II)

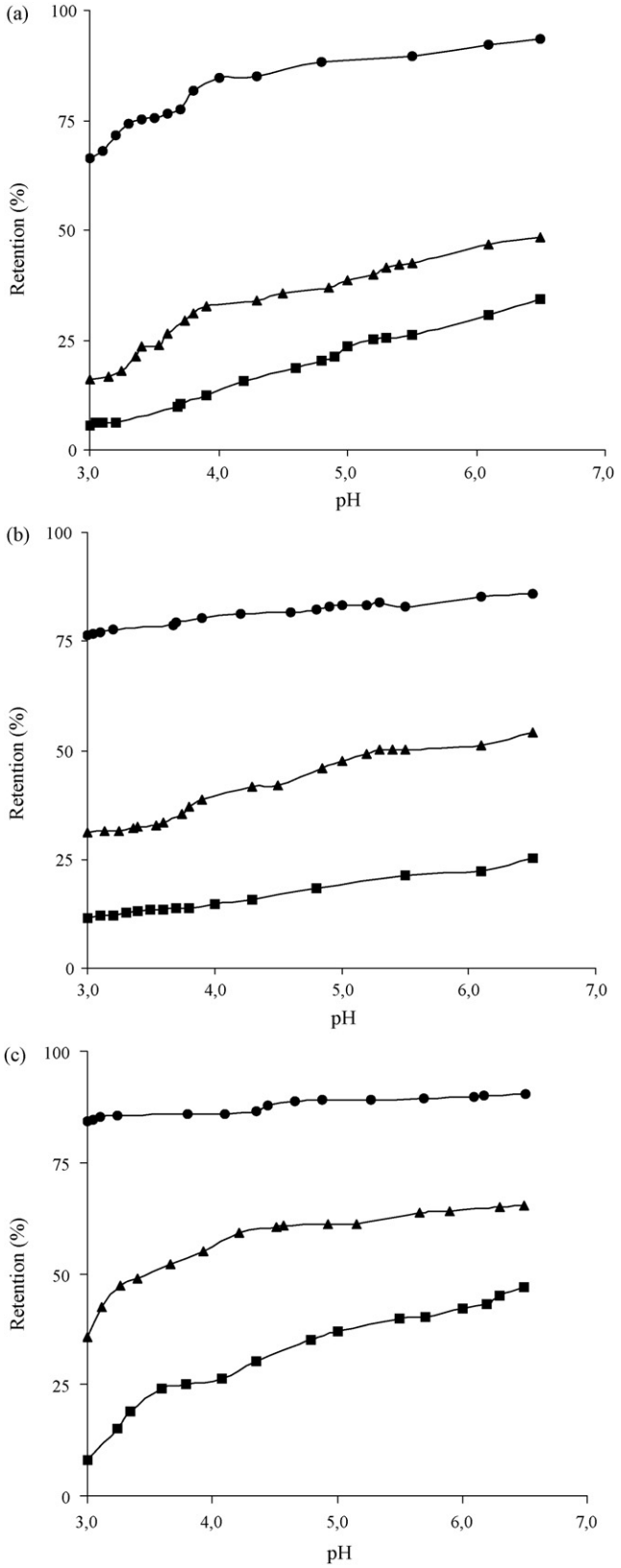

Fig. 8. (a). Adsorption of Pb(II) (20.7 mg/l) by RB (2 g/l) as function of pH and ionic strength (IS) (controlled by KNO_3), squares, 0.1 M; triangles, 0.05 M; circles, 0.01 M. (b). Adsorption of Pb(II) (20.7 mg/l) by AAB (2 g/l) as function of pH and ionic strength (IS controlled by KNO_3), squares, 0.1 M; triangles, 0.05 M; circles, 0.01 M. (c). Adsorption of Pb(II) (20.7 mg/l) by MCB (2 g/l) as function of pH and ionic strength (IS controlled by KNO_3), squares, 0.1 M; triangles, 0.05 M; circles, 0.01 M.

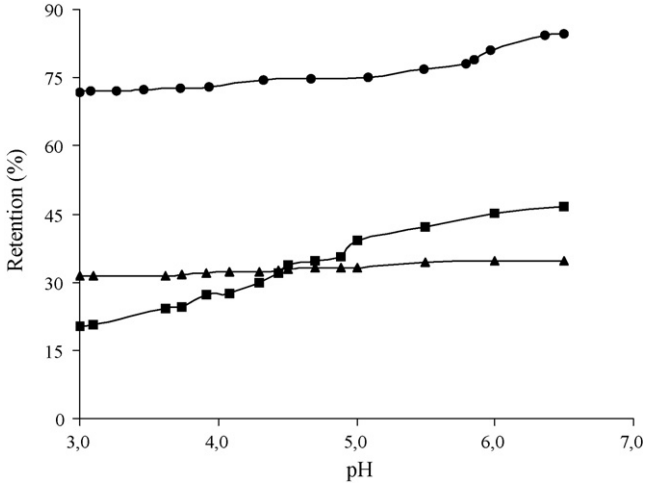

Fig. 9. Adsorption of Pb(II) (20.7 mg/l) by bentonite samples (2 g/l) as function of pH and in the presence of Cl^- [IS is 0.1 M (KNO_3)], squares, RB; triangles, AAB; circles, MCB.

onto MCB sample as a function of ionic strength and pH was shown in Fig. 8c. Increasing the ionic strength from 0.01 to 0.1 led to a significant decrease in the Pb(II) adsorption. The curves shifted to a higher pH by about 0.7–1.0 pH units when the concentration of the background electrolyte of KNO_3 increased from 0.01 to 0.1 M. The adsorption curves for MCB are characterized by two distinct adsorption edges. For example, in the presence of 0.1 M KNO_3, the first stage of adsorption edge commenced about 8% Pb(II) adsorption at pH ~3.0 and ended at pH ~3.8, at which about 25% of the total Pb(II) had been adsorbed. The second stage started at pH ~4.0 and continued up to pH 6.5 where about 48% of the total Pb(II) was adsorbed.

The adsorption of Pb(II) by the MCB sample was influenced by the presence of Cl^- (Fig. 9). It is clear that aqueous speciation influences Pb(II) adsorption in the inorganic ligand system. The adsorbed Pb(II) in the presence of inorganic ligand (Cl^-) may be also attributed to a high specificity of the surfaces for Pb(II) relative to ligand. The percent Pb(II) adsorbed in the 0.01 M Cl^- systems at pH 5.0 are 35 and 33% for the RB and AAB samples, compared to 42 and 45% at the same pH but in the absence of Cl^-. The percent Pb(II) adsorbed in the 0.1 M Cl^- system at pH 6.0 are 81% for the MCB sample, compared to 42% at the same pH but in the absence of Cl^-. These results suggest that the observed Pb(II) adsorption behavior in the bentonite suspensions is influenced by both aqueous speciation and surface ligand complexation of Pb(II) ions. The increased amount of adsorbed Pb(II) can be explained in terms of solution chemistry. Because, Pb–Cl, PbOH–Cl complexes are the dominate Pb(II) species in the presence of 0.01 M Cl^-. Thus, the specifically adsorbed ligand enhances Pb(II) retention by the surface complexation of Pb(II).

3.5. Thermodynamic studies

ΔG, ΔH° and ΔS° were evaluated for RB, AAB and MCB as −21.60 kJ/mol (at 303 K), 39 kJ/mol and 200 J/mol K, −22.63 kJ/mol (at 303 K), 41 kJ/mol and 210 J/mol K and −19.57 kJ/mol (at 303 K), 38 kJ/mol and 190 J/mol K, respectively. The negative values for the Gibbs free energy change, ΔG, show that the adsorption process for the bentonite sample is spontaneous and the degree of spontaneity of the reaction increases with increasing temperature (Table 4). The increase in adsorption with temperature may be attributed to either increase in the number of active surface sites available for adsorption on the adsorbent or the desolvation of the adsorbing species and the decrease in the thickness of the boundary layer sur-

Table 4
Thermodynamic parameters for the adsorption of Pb(II) onto bentonite samples

Sample	ΔH (kJ/mol)	ΔS (J/molK)	ΔG (kJ/mol)				R^2
			303	313	323	338	
RB	39	200	−21.60	−23.60	−25.60	−28.60	0.998
AAB	41	210	−22.63	−24.73	−26.83	−29.98	0.997
MCB	38	190	−19.57	−21.47	−23.37	−26.22	0.996

rounding the adsorbent with temperature, so that the mass transfer resistance of adsorbate in the boundary layer decreases (Table 4). These positive values of ΔH indicate the endothermic behavior of the adsorption reaction of Pb(II) ions and suggest that a large amount of heat is consumed to transfer the Pb(II) ions from aqueous into the solid phase. As was suggested by Nunes and Airoldi [34], the transition metal ions must give up a larger share of their hydration water before they could enter the smaller cavities. Such a release of water from the divalent cations would result in positive values of ΔS. This mechanism of the adsorption of Pb(II) ions is also supported by the positive values of ΔS, which show that Pb(II) ions are less hydrated in the bentonite layers than in the aqueous solution. Also, the positive value of ΔS indicates the increased disorder in the system with changes in the hydration of the adsorbing Pb(II) cations.

Similar results are reported by Sarı et al. [12] who also calculated that Gibbs free energy of Pb(II) adsorption on Celtek clay as −20.01, −19.90, −19.64 and −18.20 kJ/mol for the temperature of 293, 303, 313 and 323 K, respectively. Xu et al. [14] have found on adsorption of Pb(II) on MX-80 bentonite the temperature range of 291–328 K with ΔG increasing from −16.69 to −16.57 kJ/mol. Han et al. [31] have found that ΔH°, ΔS° and ΔG° for adsorption of Pb(II) on manganese oxide-coated sand are 18.2 kJ/mol, 117 J/K mol and −16.2 kJ/mol, respectively. Naseem and Tahir [35] have reported that ΔH°, ΔS° and ΔG° for adsorption of Pb(II) on bentonite have values of 31.74 kJ/mol, 176 J/molK and −56.67 kJ/mol, respectively. Donat et al. [36] have found that ΔH°, ΔS° and ΔG for Pb(II) adsorption on natural bentonite were reported as 26.24 kJ/mol, 133.15 J/K mol and −38.99 kJ/mol (at 293 K), respectively.

3.6. The adsorption mechanism of Pb(II)

In view of the fact pointed above, it is evident that manganese oxide modification enhanced the adsorption of Pb(II) significantly. It may be explained by considering the coordinative environments of lead ions and surface hydroxyl groups in hydrated surfaces. Surface hydroxyls may be present as bridging and terminal groups and metal centers may be coordinated with two or more hydroxyls. These differing configurations will give rise to terminal hydroxyl of different acidity [37]. Xu et al. [38] have provided evidence about mechanism of Pb(II) adsorption on amorphous hydrous Mn oxide sample. Pb(II) ions form mononuclear cornersharing surface complexes on both amorphous and crystalline Mn oxides. EXAFS analysis of Pb(II)-sorbed amorphous hydrous Mn oxide sample revealed that Pb(II) ions form mononuclear bidentate surface complexes.

4. Conclusions

- The adsorption of Pb(II) by bentonite samples was influenced by pH, ionic strength, and the presence of Cl^-. The adsorption of Pb(II) depends upon the nature of the adsorbent surface and the species distribution of Pb(II) in solution, which mainly depends on the pH of the system.
- IR spectroscopy showed that structural modification of tetrahedral sheets due to the presence of Pb(II) cations either in hexagonal holes and/or in the previously vacant octahedral sites induced changes in the Si–O vibration modes. The position and shape of the structural OH stretching bands in the IR spectra of bentonite samples was influenced by the lead cations. The findings require confirmation by direct methods such as extended X-ray absorption fine structure (EXAFS).
- The values of the adsorption coefficients indicate the favorable nature of adsorption of Pb(II) on the MCB. From the values of Langmuir monolayer capacity, q_m, it is concluded that the treatment with manganese oxide does increase the number of adsorption sites to a large extent, and the treatment also influences the strength of the existing sites as revealed by the adsorption equilibrium constant (K_L) data. The adsorption equilibrium constant (K_{L1}) of RB was higher than that of MCB. Therefore, MCB not only had a higher overall adsorption capacity than that of RB, but it also contained sites with lower binding energy for Pb(II).
- The effect of ionic strength on Pb(II) adsorption may be explained by the formation of outer-sphere complexes since K^+ in the background electrolyte could compete with the lead ions adsorbed on the outer-sphere adsorption sites and reduced the adsorption.
- The endothermic nature of the processes can be explained by the partial dehydration of Pb(II) before its adsorption on the bentonite samples.

References

[1] P.E. Marino, A. Franzblau, R. Lilis, Acute lead poisoning in construction workers: the failure of current protective standards, Arch. Environ. Health 44 (1989) 140–145.
[2] A.K. Bhattacharya, S.N. Mandal, S.K. Das, Adsorption of Zn(II) from aqueous solution by using different adsorbents, Chem. Eng. J. 123 (2006) 43–51.
[3] P.F. Luckham, S. Rossi, The colloidal and rheological properties of bentonite suspensions, Advan. Colloid Interf. Sci. 82 (1999) 43–92.
[4] E. Eren, Removal of copper ions by modified Unye clay, Turkey, J. Hazard. Mater. 159 (2008) 235–244.
[5] O. Abollino, M. Aceto, M. Malandrino, C. Sarzanini, E. Mentasti, Adsorption of heavy metals on Na-montmorillonite, Effect of pH and organic substances, Water Res. 37 (2003) 1619–1627.
[6] H.-J. Fan, P.R. Anderson, Copper and cadmium removal by Mn oxide-coated granular activated carbon, Sep. Purif. Technol. 45 (2005) 61–67.
[7] R. Dohrmann, Cation exchange capacity methodology I: An efficient model for the detection of incorrect cation exchange capacity and exchangeable cation results, Appl. Clay Sci. 34 (2006) 31–37.
[8] K. Fuda, S. Narita, Synthesis of layered transition metal oxide/clay nanocomposites., J. Ceram. Soc. Jpn 112 (2004) 717–723, Special Issue.
[9] R.W. Grimshaw, The Chemistry and Physics of Clays, Ernest Benn Ltd., London, 1971, pp. 968–979.
[10] I. Langmuir, The adsorption of gases on plane surfaces of glass, mica and platinum, J. Am. Soc. 40 (1918) 1361–1403.
[11] H. Freundlich, Über die adsorption in lösungen, Zeitschrift für Physikalische Chemie (Leipzig) 57 (1906) 385–470.
[12] A. Sarı, M. Tuzen, M. Soylak, Adsorption of Pb(II) and Cr(III) from aqueous solution on Celtek clay, J. Hazard. Mater. 144 (2007) 41–46.
[13] A. Sarı, M. Tuzen, D. Cıtak, M. Soylak, Adsorption characteristics of Cu(II) and Pb(II) onto expanded perlite from aqueous solution, J. Hazard. Mater. 148 (2007) 387–394.
[14] D. Xu, X.L. Tan, C.L. Chen, X.K. Wang, Adsorption of Pb(II) from aqueous solution to MX-80 bentonite: effect of pH, ionic strength, foreign ions and temperature, Appl. Clay Sci. 41 (2008) 37–46.
[15] A. Günay, E. Arslankaya, İ. Tosun, Lead removal from aqueous solution by natural and pretreated clinoptilolite: adsorption equilibrium and kinetics, J. Hazard. Mater. 146 (2007) 362–371.

[16] S. Veli, B. Alyüz, Adsorption of copper and zinc from aqueous solutions by using natural clay, J. Hazard. Mater. 149 (2007) 226–233.
[17] K.G. Bhattacharyya, S.S. Gupta, Adsorption of Fe(III) from water by natural and acid activated clays: studies on equilibrium isotherm, kinetics and thermodynamics of interactions, Adsorption 12 (2006) 185–204.
[18] G. Szöllösi, A. Mastalir, M. Bartok, Effect of ion exchange by an organic cation on platinum immobilization on clays, React. Kinet. Catal. Lett. 74 (2001) 241–249.
[19] T. Boonfueng, L. Axe, Y. Xu, Properties and structure of manganese oxide-coated clay, J. Colloid Interface Sci. 281 (2005) 80–92.
[20] V.C. Farmer, The layer silicates, in: V.C. Farmer (Ed.), The Infrared Spectra of Minerals, Mineralogical Society, London, 1974, pp. 331–363.
[21] J. Madejová, FTIR techniques in clay mineral studies, Vib. Spectrosc. 31 (2003) 1–10.
[22] T. Kohler, T. Armbruster, E. Libowitzky, Hydrogen bonding and Jahn–Teller distortion in groutite,α-MnOOH, and Manganite, γ-MnOOH, and their relations to the manganese dioxides Ramsdellite and Pyrolusite dioxides, J. Solid State Chem. 133 (1997) 486–500.
[23] K.M. Parida, S. Mallick, B.K. Mohapatra, N. Vibhuti, Misra, Studies on manganese-nodule leached residues: 1. Physicochemical characterization and its adsorption behavior toward Ni^{2+} in aqueous system, J. Colloid Interface Sci. 277 (2004) 48–54.
[24] J. Madejová, J. Bujdák, M. Janek, P. Komadel, Comparative FT-IR study of structural modifications during acid treatment of dioctahedral smectites and hectorite, Spectrochim. Acta Part A 54 (1998) 1397–1406.
[25] J. Madejová, B. Arvaiová, P. Komadel, FTIR spectroscopic characterization of thermally treated Cu^{2+}, Cd^{2+}, and Li^{+} montmorillonites, Spectrochim. Acta A 55 (1999) 2467–2476.
[26] J. Madejová, M. Janek, P. Komadel, H.J. Herbert, H.C. Moog, FTIR analyses of water in MX-80 bentonite compacted from high salinary salt solution systems, Appl. Clay Sci. 20 (2002) 255–271.
[27] J. Madejová, H. Pálková, P. Komadel, Behaviour of Li^{+} and Cu^{2+} in heated montmorillonite: evidence from far-, mid-, and near-IR regions, Vib. Spectrosc. 40 (2006) 80–88.
[28] E. Eren, B. Afsin, An investigation of Cu(II) adsorption by raw and acid-activated bentonite: a combined potentiometric, thermodynamic, XRD, IR, DTA study, J. Hazard. Mater. 151 (2008) 682–691.
[29] S. Zhu, H. Hou, Y. Xue, Kinetic and isothermal studies of lead ion adsorption onto bentonite, Appl. Clay Sci. 40 (2008) 171–178.
[30] S.S. Gupta, K.G. Bhattacharyya, Immobilization of Pb(II), Cd(II) and Ni(II) ions on kaolinite and montmorillonite surfaces from aqueous medium, J. Environ. Manage. 87 (2008) 46–58.
[31] R. Han, Z. Lu, W. Zou, W. Daotong, J. Shi, Y. Jiujun, Removal of copper(II) and lead(II) from aqueous solution by manganese oxide coated sand: II. Equilibrium study and competitive adsorption, J. Hazard. Mater. 137 (2006) 480–488.
[32] Y. Al-Degs, M.A.M. Khraisheh, M.F. Tutunji, Sorption of lead ions on diatomite and manganese oxides modified diatomite, Water Res. 35 (2001) 3724–3728.
[33] S.-G. Wang, W.-X. Gong, X.-W. Liu, Y.-W. Yao, B.-Y. Gao, Q.-Y. Yue, Removal of lead(II) from aqueous solution by adsorption onto manganese oxide-coated carbon nanotubes, Sep. Purif. Technol. 58 (2007) 17–23.
[34] L.M. Nunes, C. Airoldi, Some features of crystalline α-titanium hydrogenphosphate, modified sodium and *n*-butylammonium forms and thermodynamics of ionic exchange with K^{+} and Ca^{2+}, Thermochim. Acta 328 (1999) 297–305.
[35] R. Naseem, S.S. Tahir, Removal of Pb(II) from aqueous/acidic solutions by using bentonite as an adsorbent, Water Res. 35 (16) (2001) 3982–3986.
[36] R. Donat, A. Akdogan, E. Erdem, H. Cetisli, Thermodynamics of Pb2+ and Ni2+ adsorption onto natural bentonite from aqueous solutions, J. Colloid Interface Sci. 286 (2005) 43–52.
[37] P.J. Pretorius, P.W. Linder, The adsorption characteristics of δ-manganese dioxide: a collection of diffuse double layer constants for the adsorption of H^{+}, Cu^{2+}, Ni^{2+}, Zn^{2+}, Cd^{2+} and Pb^{2+}, Appl. Geochem. 16 (2001) 1067–1082.
[38] Y. Xu, T. Boonfueng, L. Axea, S. Maeng, T. Tyson, Surface complexation of Pb(II) on amorphous iron oxide and manganese oxide: spectroscopic and time studies, J. Colloid Interface Sci. 299 (2006) 28–40.